

## Structural characterization of C60 and C70 fullerenes by smallangle neutron scattering

K. A. Affholter, S. J. Henderson, G. D. Wignall, G. J. Bunick, R. E. Haufler et al.

Citation: *J. Chem. Phys.* **99**, 9224 (1993); doi: 10.1063/1.465538

View online: <http://dx.doi.org/10.1063/1.465538>

View Table of Contents: <http://jcp.aip.org/resource/1/JCPSA6/v99/i11>

Published by the [American Institute of Physics](#).

---

### Additional information on J. Chem. Phys.

Journal Homepage: <http://jcp.aip.org/>

Journal Information: [http://jcp.aip.org/about/about\\_the\\_journal](http://jcp.aip.org/about/about_the_journal)

Top downloads: [http://jcp.aip.org/features/most\\_downloaded](http://jcp.aip.org/features/most_downloaded)

Information for Authors: <http://jcp.aip.org/authors>

## ADVERTISEMENT



**Goodfellow**  
metals • ceramics • polymers • composites  
70,000 products  
450 different materials  
**small quantities fast**  
[www.goodfellowusa.com](http://www.goodfellowusa.com)

# Structural characterization of C<sub>60</sub> and C<sub>70</sub> fullerenes by small-angle neutron scattering

K. A. Affholter

*Chemical Technology Division, Oak Ridge National Laboratory, P.O. Box 2008, Oak Ridge, Tennessee 37831*

S. J. Henderson

*Biology Division, Oak Ridge National Laboratory, P.O. Box 2008, Oak Ridge, Tennessee 37831*

G. D. Wignall

*Solid State Division, Oak Ridge National Laboratory, P.O. Box 2008, Oak Ridge, Tennessee 37831*

G. J. Bunick

*Biology Division, Oak Ridge National Laboratory, P.O. Box 2008, Oak Ridge, Tennessee 37831*

R. E. Haufler and R. N. Compton

*Health and Science Research Division, Oak Ridge National Laboratory, P.O. Box 2008, Oak Ridge, Tennessee 37831*

(Received 30 April 1993; accepted 23 August 1993)

Small-angle neutron scattering (SANS) is a proven tool for examining the structure and interactions of particles in solution, though the dimensions of carbon-cage molecules are close to the lower resolution limit of the technique. Deuterated solvents (toluene-*d*<sub>8</sub> and benzene-*d*<sub>6</sub>) have virtually no scattering contrast with carbon, and the high incoherent cross section of protonated (hydrogen containing) solvents severely limits the path length of solutions by reducing the sample transmission. We have circumvented these difficulties by using CS<sub>2</sub> as a solvent which has good contrast with carbon, and a low incoherent cross section which allows the use of long sample path lengths (up to ~10 cm). In addition, CS<sub>2</sub> has good solubility for fullerenes and these properties permit the measurement of the radii of gyration (*R*<sub>g</sub>) of both C<sub>60</sub> (*R*<sub>g</sub>=3.82±0.05 Å) and C<sub>70</sub> (*R*<sub>g</sub>=4.13±0.05 Å). These dimensions are similar to those calculated from the atomic coordinates after allowing for a solvent exclusion volume. Close agreement between the measured absolute scattering cross sections and the values calculated from the particle and solvent scattering length densities serves as a cross check on the validity of this methodology. To our knowledge, this represents the first successful application of SANS for the characterization of fullerenes. SANS makes it possible to study the size and shapes of modified buckyballs, solute/solvent interactions, crystal growth from saturated solutions, and temperature dependent transitions in solutions.

## I. INTRODUCTION

The discovery that C<sub>60</sub> and C<sub>70</sub> molecules can be produced in quantity with high purity has generated significant interest in the basic and applied research communities. Potential applications are being considered in many areas (tribology, photoconductivity, nuclear medicine, superconductivity, etc.). C<sub>60</sub> and C<sub>70</sub> are two members of the class of all carbon-cage structures (fullerenes) consisting of 12 five member rings and any number of six member rings, the lowest member being the dodecahedral C<sub>20</sub> molecule. C<sub>60</sub> is known to coalesce under certain conditions into stable higher fullerenes that are multiples (C<sub>120</sub>, C<sub>180</sub>, etc.) of the initial mass.<sup>1</sup> Polymerization of C<sub>60</sub> into interconnected or dangling chains can also occur. The interaction of C<sub>60</sub> and other fullerenes with solvents has also become a topic of considerable interest. This points to the need for structural techniques that can characterize the initial particles and distinguish between individual fullerenes and aggregates of smaller fullerenes linked by single bonds or physical forces. It would also be valuable to be able to differentiate between particles of different shapes

(spherical, ellipsoidal, tubular, helical, layered structures, etc.) to probe solvent-solute and solute-solute interactions, temperature-dependent transitions in solution and the location of additional atomic species (e.g., H, K, Cl, F, Pt, Pd, Ni, U, etc.). Such information has conventionally been provided by scattering techniques<sup>2,3</sup> by measuring the intensity of a given scattered radiation (x-rays, neutrons, light, etc.) with wavelength  $\lambda$  as a function of the angle of scatter ( $2\theta$ ) or momentum transfer  $Q$

$$Q=4\pi\lambda^{-1}\sin\theta. \quad (1)$$

Typically, experiments at a given value of  $Q$  probe a distance scale  $d$ ,

$$d\simeq 2\pi/Q. \quad (2)$$

Combining Eqs. (1) and (2) gives the well-known Bragg law, which has been used for decades in the  $Q$  range  $0.6 < Q < 20 \text{ \AA}^{-1}$  to determine the structures of crystalline materials. Such experiments are conventionally referred to as wide-angle scattering and probe (atomic) distance scales [via Eq. (2)] typically in the range  $0.3 < d < 10 \text{ \AA}$ . Thus wide-angle neutron and x-ray scattering<sup>4,5</sup> have been

used to establish the dimensions, shapes, and mode of packing of fullerenes with a molecular center-to-center distance of 10.05 Å for C<sub>60</sub>.

Although Bragg's law cannot be applied to amorphous or aperiodic materials, the reciprocal or inverse relationship between real space ( $r$ ) and reciprocal space ( $Q$ ) means that Eq. (2) can be applied to first order for all types of scattering. Thus, data at lower  $Q$  values probe longer length scales in the system, and such measurements have been widely used to give structural information, typically on a length scale  $10 < d < 1000$  Å. These measurements are conventionally referred to as small-angle scattering (SAS), though it is the  $Q$  range which determines the size of objects studied [Eq. (2)] and radiations with different wavelengths can obviously provide similar information in different angular ranges. Small-angle neutron scattering and small-angle x-ray scattering (SANS and SAXS) are well established as the techniques of choice for studying the shape and interactions of particles<sup>2</sup> or molecules<sup>6</sup> in solution, though we are unaware of any applications to elucidate the morphology of fullerenes. One possible reason for the paucity of such experiments may be the fact that the dimensions of C<sub>60</sub> and C<sub>70</sub> are close to the accepted resolution limit of small-angle methodology. Thus, it is not obvious that fullerenes can satisfy the assumptions conventionally used in SAS techniques, which have no atomic resolution and are typically applied to groups of atoms, for which one can define an average scattering power [e.g., the electron density (ED) for SAXS]. For SANS, the equivalent parameter is the scattering length density (SLD) which is the sum of coherent neutron scattering lengths ( $b_{\text{coh}}$ ) over all atoms in a given volume ( $\Delta V$ ) divided by  $\Delta V$ .<sup>6,7</sup> The scattered intensity ( $I$ ) is proportional to the contrast [i.e., the square of the difference in scattering power (SLD or ED) between the particle and solvent], and a comparison of the measured and calculated (theoretical) absolute scattering cross section can be used as a cross check on the validity of the method. Such comparisons lead to excellent agreement in studies of polymer latex morphology<sup>8</sup> on length scales  $\sim 500$ – $1000$  Å. However, it has not hitherto been demonstrated that these concepts can be applied on the size range exhibited by fullerenes, or that the number of atoms involved is sufficient to define an average SLD or ED, which remains constant over the size range probed. We have therefore performed experiments to explore the validity of this methodology on C<sub>60</sub> and C<sub>70</sub>, because if SAS concepts can be shown to apply to such small numbers of atoms, they can clearly be applied to higher fullerenes.

In addition, in a SAS experiment, the intensity is known<sup>2,9</sup> to be a strong function of the particle dimensions ( $I \sim R^6$ ), so that such small particles will have extremely low scattering cross sections compared to the inherent (e.g., incoherent) and instrumental background signals. Thus, all other experimental parameters (concentration, scattering contrast, backgrounds, etc.) must be optimized to give a measurable signal. We have therefore chosen initially to concentrate on SANS because the ratio of scattering to absorption for several elements (e.g., cadmium and

boron) is virtually zero, so that neutron beams can be very well collimated with very little parasitic scattering from the slits or sample container. For SAXS, on the other hand, materials which have high absorption (to define a SAXS beam) also have high scattering power, as both parameters are a strong function of the atomic number and parasitic scattering is usually much higher for SAXS.

Also, there are several materials which can be used for sample containment (e.g., quartz), which have very little absorption or scattering for neutrons, although it is much harder to contain samples in a SAXS camera as most materials have substantial absorption, which attenuates the beam. Thus, the high penetrating power of neutrons makes it relatively easy to contain samples with a minimum of instrumental backgrounds and to use long sample path lengths to maximize the scattered intensity. Moreover, the differences in scattering power which may be introduced by isotopic substitution<sup>6,9</sup> give more freedom to optimize the signal-to-noise ratio of the experiment by a suitable choice of the isotopic components. Finally, SANS absolute calibration<sup>10</sup> allows a comparison of the measured and theoretical cross sections to serve as a cross check of the validity of the overall approach. This paper will therefore explore the utility of SANS for structural determinations of fullerenes, though SAXS may also be an important technique for characterizing endohedral or exohedral fullerenes which have been doped with heavy elements, thus giving rise to ED contrast. Such experiments are also in progress and will be the subject of a forthcoming publication.

## II. SAMPLE SELECTION AND PREPARATION

C<sub>60</sub> is known<sup>11</sup> to have limited solubility in a number of organic solvents including benzene (1.7 mg/ml), toluene (2.8 mg/ml), xylene (5.2 mg/ml), and CS<sub>2</sub> (7.9 mg/ml), and the highest reported solubility is in chloronaphthalene (50 mg/ml). Protonated solvents (i.e., those containing hydrogen atoms) give rise to high background scattering due to the large incoherent cross sections ( $\sigma_{\text{inc}} \sim 80$  barns; 1 barn =  $10^{-24}$  cm<sup>2</sup>). The precise magnitude of  $\sigma_{\text{inc}}$  for H<sup>1</sup> is a function of wavelength,<sup>6,12</sup> temperature,<sup>12</sup> and even the particular chemical group in which it is situated.<sup>13</sup> However, it is always an order of magnitude higher than the incoherent cross sections<sup>6</sup> of other isotopes (e.g.,  $\sigma_{\text{inc}} \approx 0.01$  barns for S<sup>32</sup>;  $\sigma_{\text{inc}} \approx 2.0$  barns for D<sup>2</sup>) or naturally occurring elements (e.g.,  $\sigma_{\text{inc}} < 0.02$  barns for C;  $\sigma_{\text{inc}} \approx 5.9$  barns for Cl, etc.) contained in the above solvents.

In order to optimize the signal-to-noise ratio of a SANS experiment, it is necessary to satisfy several conditions simultaneously. First, there must be good scattering contrast between the particle and solvent (Table I) and the concentration must be maximized, consistent with the requirement that the particles scatter as individual entities (i.e., no measurable particle-particle interactions). This may be confirmed by checking that the intensity scales linearly with the concentration ( $C$ ). Second, the scattering is proportional<sup>2,9</sup> to the product of the sample transmission ( $T$ ) and thickness ( $t$ ), and is optimized for maximum intensity when  $\mu t = 1$ , where  $\mu$  is the linear attenuation coefficient ( $T = e^{-\mu t}$ ). This condition allows as much sam-

TABLE I. Comparison of the relative scattering powers of C<sub>60</sub> in various solvents.

Solvent	Maximum solubility C <sub>60</sub> (mg/ml) <sup>a</sup>	Scattering length density of solvent $\rho$ (10 <sup>10</sup> cm <sup>-2</sup> )	Relative scattering power $C[\rho(C_{60})^b - \rho_{\text{solvent}}]^2$ (mg/ml) (10 <sup>20</sup> cm <sup>-2</sup> )
Carbon disulfide	7.9	1.24	313
Chloronaphthalene- <i>d</i> <sub>7</sub>	51.0	5.20	276
Xylene- <i>d</i> <sub>10</sub>	5.2	6.04	12
Toluene- <i>d</i> <sub>8</sub>	2.8	5.66	10
Benzene- <i>d</i> <sub>6</sub>	1.7	5.42	8

<sup>a</sup>Ruoff *et al.* (Ref. 11) report solubilities for C<sub>60</sub> in protonated solvents.

<sup>b</sup> $\rho(C_{60}) = 7.53 \times 10^{10} \text{ cm}^{-2}$  using a volume calculated from the van der Waals radii of the crystal 5.02 Å.

ple as possible in the path of neutrons, consistent with attenuation of the beam, and can raise the scattered intensity for nonprotonated solvents as compared to their protonated equivalents. The use of such solvents has the added advantage of minimizing the incoherent background. However, the deuterated counterparts of most of the available solvents have virtually no scattering contrast with carbon (Table I) and we have therefore chosen CS<sub>2</sub> as the material which comes closest to satisfying these criteria.

Pure C<sub>60</sub> (99 wt.%) and pure C<sub>70</sub> (98 wt.%) were obtained from Texas Fullerenes Inc., Houston, Texas. The samples were produced with an arc fullerene generator<sup>14</sup> and extracted from the soot with toluene. The residual toluene was removed by washing the fullerene crystals with diethyl ether and the mixture was then purified using column chromatography. CS<sub>2</sub> was reagent grade (99.98%). Two nominal concentrations of approximately 5 and 8 mg/ml (the highest recorded<sup>11</sup> concentration in CS<sub>2</sub>) were made up for both C<sub>60</sub> and C<sub>70</sub> to check that particle dimensions were independent of the concentration and that the scattering cross section scaled linearly with *C*. The actual concentrations, measured after each scattering experiment, were slightly different due to precipitation, etc. These are given to three significant figures in Sec. III and were used in the comparisons with theory, though the nominal concentrations are used as round numbers for descriptive purposes (e.g., in Fig. 2).

Seventy-five milligrams of C<sub>60</sub> (or C<sub>70</sub>) were added to 7.5 ml CS<sub>2</sub> and the sample was stirred and then placed in an ultrasound cleaning bath for an additional 5 min. The sample was removed, placed in six separate eppendorfs, spun (8000 rpm) for 2 min, and carefully decanted and inserted in a 20 mm path length quartz cell, leaving the sediment behind. A Teflon cap was placed in the small opening at the top of the quartz cell and this was sealed with plastic wrap.

### III. SANS EXPERIMENTS

The experiments were performed on the W. C. Koehler 30 m SANS facility at the Oak Ridge National Laboratory.<sup>15</sup> The neutron wavelength was 4.75 Å ( $\Delta\lambda/\lambda \sim 5\%$ ) and the beam was transported to a distance of 1.5 m from

the sample by means of moveable neutron guides. The source and sample Cd slits (irises) were 3.5 and 1.6 cm in diameter, respectively, and the sample-detector distance was 1.55 m. The samples were contained in quartz cells with a path length of 20 mm and the area detector was a 64 × 64 cm<sup>2</sup> proportional counter with element size  $\sim 1 \text{ cm}^2$ . The data were corrected on an element-by-element basis for the detector efficiency and instrumental and solvent backgrounds prior to radial averaging in the *Q* range  $0.05 < Q < 0.40 \text{ Å}^{-1}$ . The solvent and instrumental background formed only a small correction to the sample (fullerene) data and the net intensities were converted to an absolute ( $\pm 4\%$ ) differential cross section per unit sample volume [ $d\Sigma/d\Omega(Q)$  in units of cm<sup>-1</sup>] by comparison with precalibrated secondary standards based on the measurement of beam flux, vanadium incoherent cross section, the scattering from water, and other reference materials.<sup>10</sup> The efficiency calibration was based on the scattering from light water and led to angle-independent scattering for vanadium, H-polymer blanks, and water samples of different thicknesses.

The transmission of the sample was measured in a separate experiment<sup>16</sup> by collimating the beam with slits (irises)  $\sim 1 \text{ cm}$  in diameter, separated by a distance  $\sim 7.5 \text{ m}$ . A strongly scattering sample, porous carbon, was placed at the sample position to spread the beam over the detector, placed at a sample-detector distance  $\sim 10 \text{ m}$ . Without the carbon in position, the beam would either be blocked by the beam stop or be concentrated in a few detector cells, with the possibility of saturating or damaging the detector. The total count summed over the whole detector ( $> 10^5$ ) was recorded in a time period  $\sim 1 \text{ min}$  and the sample being measured was placed over the source slit, thus attenuating the beam. The count was repeated over the same time interval and the transmission is given by the ratio of the two counts after minor corrections ( $< 0.1\%$ ) for the beam-blocked background due to electronic noise, cosmic rays, etc. In this geometry, no scattering from the sample at *Q* values  $> 10^{-3} \text{ Å}^{-1}$  can enter the second iris and be rescattered by the porous carbon and hence be counted by the detector. All measurements were performed at room temperature ( $T = 23^\circ \text{C}$ ) and typical values of the empty quartz cell and sample transmissions were  $T = 0.95$  and  $T = 0.77$  for a 20 mm path length. The use of 20 mm cells increased the signal by approximately an order of magnitude, as compared with the more commonly used 1–2 mm path length cells. Typical run times were in the range 1–4 h. After each SANS experiment, a portion of the solution was removed from the quartz cell and sealed in a glass ampoule for later quantification. The quantification was made via spectrophotometry using the fullerene molar extinction coefficients.<sup>17</sup> Each sample was quantified using at least 20 wavelength data points to establish the concentration of the scanned solution. These were prepared by sampling a known volume of the SANS samples, allowing the solvent to dry, and redissolving in toluene of a known volume. The concentration (*C*) of the “8 mg/ml” C<sub>60</sub> preparation was 7.75 mg/ml and the “5 mg/ml” preparation measured 5.45 mg/ml; the concentra-

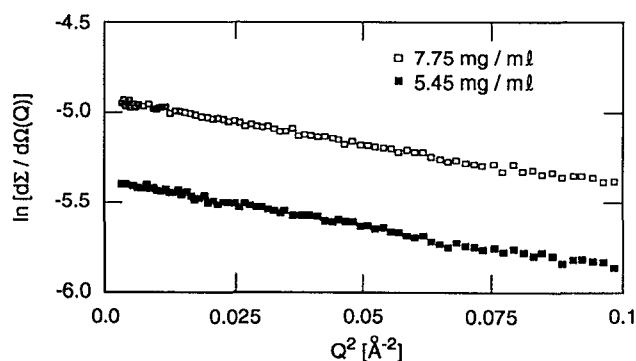


FIG. 1. Guinier plots [ $\ln d\Sigma/d\Omega(Q)$  vs  $Q^2$ ] for  $C_{60}$  fullerenes at two different concentrations.

tion of the 8 mg/ml  $C_{70}$  preparation was 7.59 mg/ml and the 5 mg/ml preparation gave 4.78 mg/ml.

#### IV. RESULTS

The Guinier approximation<sup>2</sup> for independently scattering particles is

$$\frac{d\Sigma}{d\Omega}(Q) = \frac{d\Sigma}{d\Omega}(0) \exp\left[-\frac{(Q^2 R_g^2)}{3}\right], \quad (3)$$

where  $d\Sigma/d\Omega(Q)$  is the differential scattering cross section per unit solid angle per unit sample volume (in units of  $\text{cm}^{-1}$ ) and  $R_g$  is the radius of gyration [i.e., the root-mean-square (r.m.s.) distance of all scattering elements from the center of gravity]. Figure 1 shows Guinier plots [ $\ln(d\Sigma/d\Omega)$  vs  $Q^2$ ] for  $C_{60}$  in  $\text{CS}_2$  at nominal concentrations of 5 and 8 mg/ml, and it may be seen that each has the same slope within the statistical errors. Similar plots were given for the  $C_{70}$  particles, where the slopes are again independent of concentration. However, the average slope is quite different for the two moieties as indicated in Fig. 2, which compares the 8 mg/ml data for  $C_{60}$  and  $C_{70}$ . All the plots have linear regions whose zero- $Q$  intercept and slope can be analyzed<sup>2,6,9</sup> to give the extrapolated cross section  $d\Sigma/d\Omega(0)$  and  $R_g$ , respectively. It may easily be seen that the  $C_{70}$  particles have a higher slope (and hence higher  $R_g$ ) than the  $C_{60}$  fullerenes. Despite the very low cross section

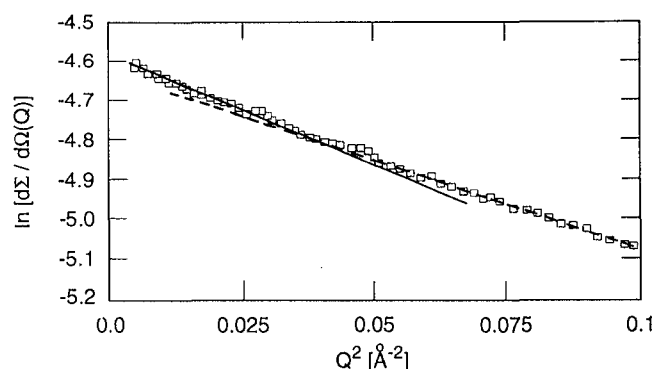


FIG. 3. A Guinier plot for a mixture of  $C_{60}$  (7.4 mg/ml) and  $C_{70}$  (5.1 mg/ml) fullerenes in  $\text{CS}_2$ .

[ $d\Sigma/d\Omega(0) \sim 10^{-2} \text{ cm}^{-1}$  for  $C \sim 8 \text{ mg/ml}$ ], the careful attention given to optimizing the signal to noise ratio resulted in very high net count rates ( $\sim 300\text{--}500 \text{ Hz}$  for  $C \sim 5\text{--}8 \text{ mg/ml}$ ).

At some value of  $Q$ , the data will depart from the Guinier law [Eq. (3)], so different values of  $Q_{\text{max}}$  were used in the least-squares linear regression. Changing  $Q_{\text{max}}$  from 0.22 to  $0.31 \text{ Å}^{-1}$  produced relatively little difference in  $R_g$  (e.g., 3.83 and  $3.84 \text{ Å}$  for  $C_{60}$ ; 4.14 and  $4.13 \text{ Å}$  for  $C_{70}$ ). This allowed the use of large numbers of experimental points in the linear regression ( $> 50$  for  $Q_{\text{max}} = 0.022 \text{ Å}$  and  $> 80$  for  $Q_{\text{max}} = 0.031 \text{ Å}$ ) and led to very small statistical errors for both concentrations ( $\sim \pm 0.02 \text{ Å}$ ). Similarly, the  $R_g$  values for the 5 and 8 mg/ml samples show virtually no systematic concentration dependence (3.85 and  $3.80 \text{ Å}$ , respectively, for  $C_{60}$ ; 4.10 and  $4.14 \text{ Å}$ , respectively, for  $C_{70}$ ). Thus the  $R_g$  values for the two different concentrations and  $Q_{\text{max}}$  limits were averaged to give  $3.82 \pm 0.05 \text{ Å}$  for  $C_{60}$  and  $4.13 \pm 0.05 \text{ Å}$  for  $C_{70}$ , where the error represents the sum of statistical and systematic errors. Figure 3 shows the Guinier plot of a mixture of  $C_{60}$  (7.4 mg/ml) and  $C_{70}$  (5.08 mg/ml) in  $\text{CS}_2$ . In contrast to the pure components (Figs. 1 and 2), two slopes are clearly seen and thus SANS seems to be able to differentiate between pure fullerenes and mixtures. However, it would be necessary to analyze the latter data in terms of two superimposed exponential functions (rather than taking the limiting slopes as in Fig. 3) to determine the precise  $R_g$ 's of each component of the mixture.

For a homogeneous particle suspended in a solvent medium, the neutron scattering cross section at  $Q=0$  is given<sup>8</sup> by

$$\frac{d\Sigma}{d\Omega}(0) = (\rho_p - \rho_{\text{solvent}})^2 N_p V_p^2, \quad (4)$$

where  $\rho_p$  and  $\rho_{\text{solvent}}$  are the scattering length densities of the particle and solvent, respectively,  $N_p$  is the number of particles per unit volume, and  $V_p$  is the particle volume. We have assumed initially that there are no particle-solvent and/or particle-particle interactions which would give rise to a finite second virial coefficient and introduce an extra concentration dependent term<sup>2,9</sup> into Eqs. (3) and (4).

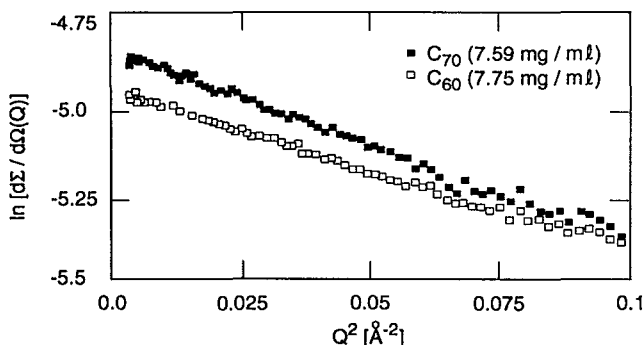


FIG. 2. Guinier plots [ $\ln d\Sigma/d\Omega(Q)$  vs  $Q^2$ ] for  $C_{60}$  and  $C_{70}$  fullerenes at a nominal concentration of 8 mg/ml.

TABLE II. A comparison of measured and calculated dimensions and cross sections for  $C_{60}$  and  $C_{70}$  fullerenes.

	$C_{60}$ 7.75 mg/ml	$C_{60}$ 5.45 mg/ml	$C_{70}$ 7.59 mg/ml	$C_{70}$ 4.78 mg/ml
$R_g(\text{\AA})$ (experiment)	3.80	3.85	4.14	4.10
$R_g(\text{\AA})$ (model)	3.74	3.74	4.16	4.16
$10^3 d\Sigma/d\Omega(0)$ ( $\text{cm}^{-1}$ ) (experiment)	7.20	4.61	8.11	4.18
$10^3 d\Sigma/d\Omega(0)$ ( $\text{cm}^{-1}$ ) (theory)	7.21	5.07	8.07	5.08

For large particles (e.g., polymer latexes), it is easy to define a SLD using the bulk polymer density.<sup>7,8</sup> However, for fullerenes, the concept of SLD cannot be applied over distances  $\sim 1$  Å as the density is not uniform. We have assumed that the smallest length scale on which the concept might apply is  $\sim 5$  Å, and to test this hypothesis, we have calculated the theoretical cross sections for each concentration, assuming a two phase system with effective particle volumes of  $530 \text{ \AA}^3$  ( $C_{60}$ ) and  $650 \text{ \AA}^3$  ( $C_{70}$ ) from which the  $\text{CS}_2$  molecules are excluded. The former volume is calculated from the van der Waals radius ( $5.02 \text{ \AA}$ ) and the latter from the dimensions<sup>19</sup> of  $C_{70}$ . The particle SLD is calculated by assuming that the 60 (or 70) carbon atoms (each with a coherent scattering length of  $0.665 \times 10^{-12} \text{ cm}$ ) are distributed over the appropriate volume (Table I). This gives the theoretical values shown in Table II, which are in remarkably good agreement with the experimental (extrapolated) cross sections for both  $C_{60}$  and  $C_{70}$  fullerenes. This agreement supports the assumption that particle-solvent interactions may be neglected to a good approximation. We plan to further explore the validity of this hypothesis in a future publication by conducting measurements over a wider range of concentration.

## V. DISCUSSION

The r.m.s. distance of all scattering elements from the center of gravity ( $R_g$ ) can be easily calculated for simple geometrical bodies such as hollow spheres and ellipsoids with known inner and outer radii. We used the atomic coordinates given in Refs. 18 and 19 in conjunction with a Monte Carlo (MC) shape modeling program,<sup>20</sup> which was designed to calculate  $I(Q)$  profiles for various geometrical shapes. This led to values of  $3.70$  and  $4.13 \text{ \AA}$  for  $C_{60}$  and  $C_{70}$  carbon shells, respectively, though these values are reduced by including a solvent exclusion volume, which decreased them to  $3.67$  and  $4.09 \text{ \AA}$ , respectively. These estimates may be compared with experimental values of  $3.82$  and  $4.13 \text{ \AA}$ , which are slightly ( $\sim 2\%$ ) higher. A discrepancy of this order is not unexpected as it is well known that the true  $R_g$  applies only in the limit of  $QR_g \rightarrow 0$  and that slightly higher values are expected for finite  $QR_g$ . For  $(QR_g)_{\text{max}} \approx 0.8$ , the perturbation may be estimated<sup>21</sup> to be  $\sim 2\%$ – $5\%$  for Gaussian coils and solid spheres, respectively, whereas an estimate of  $1.8\%$  ( $0.07 \text{ \AA}$ ) was obtained for a shell via the MC modeling program<sup>20</sup> for a shell morphology. Thus, the observed dimensions are very close ( $\pm 0.5\%$ ) to those estimated from the known structure of fullerenes (see Table II). This lends strong support to the

idea that SANS can accurately characterize the dimensions of such particles, along with any changes introduced by atomic substitution, polymerization, processing, etc.

Indirect Fourier transform analysis<sup>22</sup> of the SANS data reveals a maximum intraparticle distance  $D_{\text{max}} \sim 12 \text{ \AA}$  ( $C_{60}$ ) and  $11.5 \text{ \AA}$  ( $C_{70}$ ) and these distances are also consistent with the concept of a solvent exclusion volume. This methodology also yields the length distribution function for the particle and will be explored in more detail in a forthcoming publication.

## VI. CONCLUSIONS

SANS appears to be an especially promising technique for characterizing fullerenes. Although the measured dimensions are close to the accepted resolution limit of the technique, the excellent agreement between the experimental and calculated dimensions gives strong support to the hypothesis that individual fullerene particles containing as few as 60–70 atoms can be resolved. In addition to the particle dimensions, the theoretical and experimental cross sections are in excellent agreement despite the extreme sensitivity of the calculation to both the assumed dimensions ( $I \sim R^6$ ) and scattering length densities ( $I \sim \Delta\rho^2$ ). The fact that SAS concepts can be successfully applied on such a small length scale gives reasonable expectations that the SANS technique will prove to be even more useful as applied to higher fullerenes and their derivatives. Such experiments are currently in progress.

## ACKNOWLEDGMENTS

We are grateful to B. Chakoumakos for helpful discussions, R. L. Hettich and C. Jin for performing the mass spectrometry on the samples employed, and M. Segman and P. Brett for providing solvents. We also wish to acknowledge helpful discussions with S. Spooner and D. Svergun concerning the molecular modeling. The research was sponsored by the Directors R&D Fund, the Office of Health and Environmental Research, and the Division of Materials Sciences, U. S. Department of Energy under Contract No. DE-AC05-84OR21400 with Martin Marietta Energy Systems Inc.

<sup>1</sup> (a) Y. Chai, T. Guo, R. E. Haufler, L. P. F. Chibante, J. Fure, L. Wang, J. M. Alford, and R. E. Smalley, *J. Phys. Chem.* **95**, 7564 (1991); (b) R. L. Whetton, C. Yeretian, and K. Hansen, *Nature* **359**, 44 (1992).

<sup>2</sup> A. Guinier and G. Fournet, *Small-Angle Scattering of X-rays* (Wiley, New York, 1955).

- <sup>3</sup>B. E. Warren, *X-ray Diffraction* (Addison-Wesley, Reading, MA, 1969).
- <sup>4</sup>W. I. F. David, R. M. Ibberson, R. J. S. Dennis, J. P. Hare, and K. Prassides, *Europhys. Lett.* **18**, 219 (1992).
- <sup>5</sup>W. Kratschmer, L. D. Lamb, K. Fostiropoulos, and D. R. Huffman, *Nature* **347**, 354 (1990).
- <sup>6</sup>G. D. Wignall, *Encyclopedia of Polymer Science and Engineering*, edited by M. Grayson and J. Kroschwitz (Wiley, New York, 1978), Vol. 10, p. 112.
- <sup>7</sup>J. B. Hayter, in *Proceedings of Enrico Fermi School of Physics Course, XC*, edited by V. Degiorgio and M. Corti (North Holland, Amsterdam, 1985), p. 59.
- <sup>8</sup>G. D. Wignall *et al.*, *Mol. Cryst. Liq. Cryst. A* **180**, 25, (1990).
- <sup>9</sup>*Neutron, X-Ray and Light Scattering*, edited by P. Lindner and T. Zemb, (Elsevier, New York, 1991).
- <sup>10</sup>G. D. Wignall and F. S. Bates, *J. Appl. Cryst.* **20**, 28 (1986).
- <sup>11</sup>R. S. Ruoff, D. S. Tse, R. Malhotra, and D. C. R. Lorentz, *J. Phys. Chem.* **97**, 3379 (1993).
- <sup>12</sup>A. Maconnachie, *Polymer* **25**, 1068 (1984).
- <sup>13</sup>L. D. Coyne and W. Wu, *Polymer Commun.* **30**, 312 (1989).
- <sup>14</sup>R. E. Haufler *et al.*, *J. Phys. Chem.* **94**, 8634 (1990).
- <sup>15</sup>W. C. Koehler, *Physica (Utrecht) B* **137**, 320 (1986).
- <sup>16</sup>W. S. Dubner, J. M. Schultz, and G. D. Wignall, *J. Appl. Cryst.* **23**, 469 (1990).
- <sup>17</sup>M. Diack, R. E. Haufler, R. N. Compton, and G. Guiochon, *Anal. Chem.* (submitted).
- <sup>18</sup>R. M. Fleming *et al.* *Mater. Res. Symp. Proc.* **206**, 691 (1991).
- <sup>19</sup>D. R. McKenzie, C. A. Davis, D. J. H. Cockayne, D. A. Muller, and A. M. Vassallo, *Nature* **355**, 622 (1992).
- <sup>20</sup>S. J. Henderson, *J. Appl. Cryst.* (to be published).
- <sup>21</sup>D. I. Svergun, A. V. Semenyuk, and L. A. Feigin, *Acta. Crystallogr. Sect A* **44**, 244 (1988).
- <sup>22</sup>R. J. Ullman, *J. Polymer. Sci., Polymer. Lett.* **21**, 521 (1983).